

Robust and Electron-Rich *cis*-Palladium(II) Complexes with Phosphine and Carbene Ligands as Catalytic Precursors in Suzuki Coupling Reactions

Chuang-Yi Liao, Kai-Ting Chan, Cheng-Yi Tu, Yu-Wei Chang, Ching-Han Hu, and Hon Man Lee*^[a]

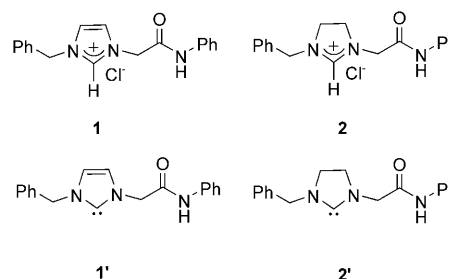
Abstract: A new imidazolium ligand precursor $[L^2H]Cl$ (**2**) was prepared in 86% yield. Compared with its imidazolium counterpart, $[L^1H]Cl$ (**1**), **2** is very sensitive to moisture and can undergo ring-opening reactions very readily. Palladium complexes with the ring-opened products from imidazolium salts were isolated and characterized by X-ray crystallography. Theoretical studies confirmed that the imidazolium salt has a higher propensity for the ring-opening reaction than the imidazolium counterpart. New mixed phosphine/carbene palladium complexes, *cis*- $[PdCl_2(L)(PR_3)]$ ($L=L^1$ and L^2 ; $R=Ph, Cy$), were successfully prepared. These complexes are highly robust as revealed by variable-temperature NMR spectroscopic studies and thermal gravimetric analysis. The structural and electronic properties of the new complexes on varying the carbene

group (imidazol-2-ylidene group (unsaturated carbene) vs. imidazolin-2-ylidene (saturated carbene)) and the phosphine group (PPh_3 vs. PCy_3) were studied in detail by X-ray crystallography, X-ray photoelectron spectroscopy, and theoretical calculations. The catalytic study reveals that *cis*- $[PdCl_2(L^2)-(PCy_3)]$ is a competent Pd^{II} precatalyst for Suzuki coupling reactions, in which unreactive aryl chlorides can be applied as substrates.

Keywords: aryl chlorides • carbene ligands • cross-coupling • palladium • phosphine ligands

Introduction

Nowadays, *N*-heterocyclic carbenes (NHCs) are ubiquitous in the literature because of their great applicability in diverse catalytic reactions,^[1,2] such as cross-coupling reactions,^[3–5] olefin metathesis,^[6] hydrosilylation,^[7] and polymerization^[8]. Biomedical applications based on NHCs are also being developed.^[9,10] Despite their wide use, factors governing their reactivity are still not fully understood.^[11,12] Over the past few years, our group and others have been focusing on the development of functionalized NHCs.^[13,14] In previous contributions, we published chelate and nonchelate palladium complexes^[15] as well as their nickel^[16] and silver^[17] complexes based on the ligand precursor **1**. The monodentate NHC (**1'**) derived from **1** contains an imidazol-2-ylidene



(unsaturated NHC) moiety. It has been shown that NHC ligands based on imidazolin-2-ylidene (saturated NHC) gave superior coupling activities than the unsaturated analogues,^[18] which may be related to the higher donor ability of the former ligand.^[19] For reactions catalyzed by late-transition-metal complexes, the increased donor ability of the ligand may play an important role in bond activation. Therefore, we have been investigating the transition-metal complexes with the saturated carbene ligand (**2'**) derived from the ligand precursor **2**.

Functionalized NHC ligands have been attracting much interest.^[14,20–22] It has been shown by others^[23–26] and ourselves^[27,28] that palladium or nickel complexes with multi-

[a] C.-Y. Liao, K.-T. Chan, C.-Y. Tu, Y.-W. Chang, Prof. Dr. C.-H. Hu, Prof. Dr. H. M. Lee
Department of Chemistry
National Changhua University of Education
Changhua, 50058 (Taiwan)
Fax: (+886)4-7211190
E-mail: leehm@cc.ncue.edu.tw

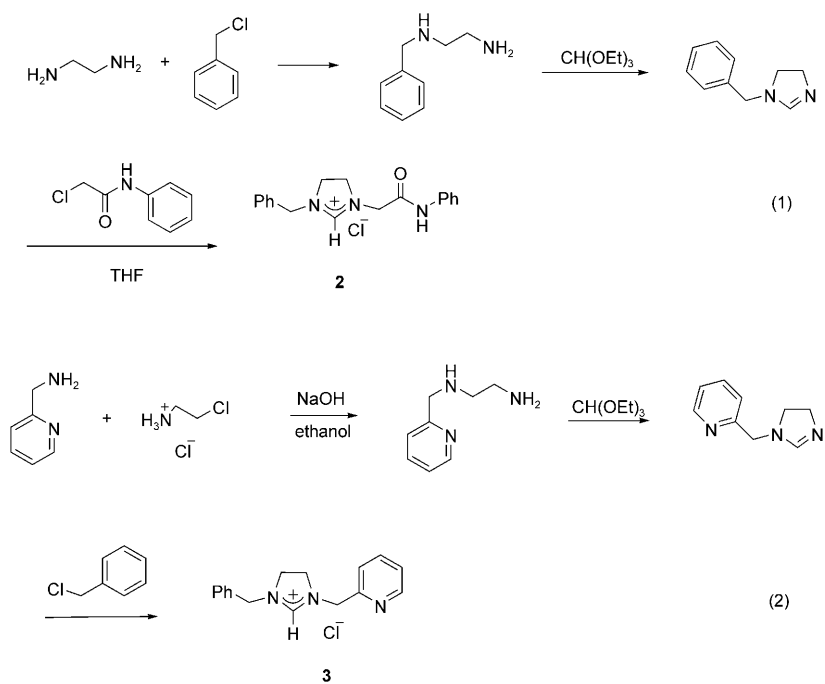
Supporting information for this article is available on the WWW under <http://dx.doi.org/10.1002/chem.200801296>.

dentate ligands containing NHC and phosphine groups are effective catalysts for C–C coupling reactions. The mixed donor ligand is believed to be hemilabile; the carbene group binds to the metal by a strong σ bond, whereas the phosphine group is labile; vacant coordination sites are available for substrates through phosphine dissociation. Theoretical calculations by Rösch et al.^[29] have also shown that a palladium complex with a bidentate phosphine/NHC ligand was a suitable catalyst for Heck reactions; and during the course of reaction, the Pd–P bond was reversibly broken. However, instead of synthesizing multi-dentate phosphine/carbene ligands, the use of monodentate phosphine co-ligands of different electronic and steric properties should allow fine-tuning of palladium(II) NHC complexes in a more facile fashion. An earlier work by Hermann and et al. indicated that $[\text{PdI}_2(\text{NHC})(\text{PR}_3)]$ is effective in C–C coupling activities.^[30]

In this contribution, we report our successful preparation of a new saturated NHC precursor and a systematic investigation on the ligand properties between the saturated and the unsaturated NHCs. Notably, we found that the introduction of bulky, electron-donating PCy_3 as the co-ligand creates a highly electron-rich yet thermally stable *cis*- $[\text{PdCl}_2(\text{NHC})(\text{PR}_3)]$ precatalysts that display effective Suzuki coupling activities. In the course of our investigation, we also noted, in sharp contrast to **1**, the high sensitivity of **2** towards water to form ring-opened products. The mechanistic aspects of this ring-opening reaction is examined with the help of theoretical calculations.

Results and Discussion

Preparation of ligand precursors: The imidazolium carbene precursor **1** was previously prepared by us.^[15] Scheme 1 shows the synthetic routes for the imidazolium precursors **2** and **3**. The intermediate, 1-benzyl-4,5-dihydroimidazole, was prepared from the cyclization reaction between triethylorthoformate and *N*-benzylethylenediamine, the latter of which was obtained easily by refluxing a mixture of 1,2-ethanediamine and benzyl chloride. A simple quaternization reaction between the dihydroimidazole and 2-chloro-*N*-phenylacetamide afforded **2** in a pure form in 86% yield. The synthetic route for **3** is similar to that for **2**. A reaction between 2-(aminomethyl)pyridine and 2-chloroethylamine



Scheme 1.

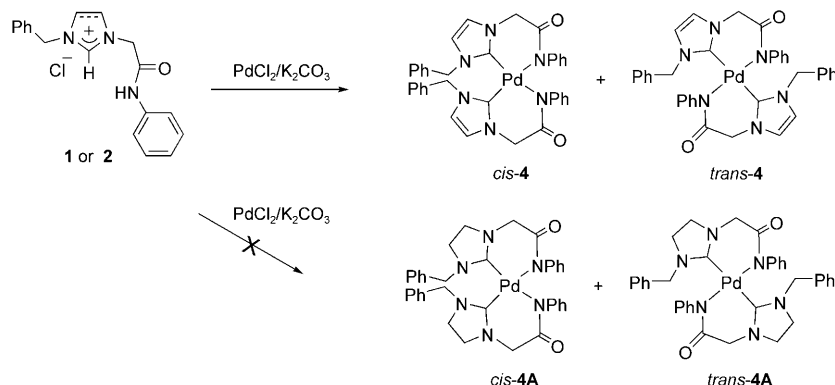
monohydrochloride under basic conditions afforded *N'*-(pyridin-2-ylmethyl)ethane-1,2-diamine,^[31] which was then treated with triethylorthoformate to produce 2-(4,5-dihydro-1*H*-imidazol-1-yl)methyl-pyridine. A similar quaternization reaction between the dihydroimidazole and benzyl chloride gave the imidazolium salt **3** in 72% yield.

A comparison of the $^{13}\text{C}\{^1\text{H}\}$ NMR spectra between **1** and **2** reveals an interesting aspect. The NCN signal in **1** resonates at $\delta = 138.0$ ppm, whereas the corresponding signal in **2** resonates at $\delta = 161.1$ ppm. A search of the literature indicates that the downfield shift of the C2 resonance from imidazolium to imidazolium compounds is a general phenomenon.^[32,33] For example, Plenio et al. reported the ^{13}C NMR spectroscopic data for *N,N'*-bis(2,6-dimethyl-4-diethylaminophenyl)imidazolium chloride and *N,N'*-bis(2,6-dimethyl-4-diethylaminophenyl)imidazolium chloride.^[33] The C2 carbon atom of the former compound resonates at $\delta = 139.2$ ppm, whereas the corresponding signal for the latter compound was observed at $\delta = 160.8$ ppm. Intriguingly, the drastic downfield shift of $\delta = 23.1$ ppm for the C2 carbon atom may correlate with the difference in reactivity between **1** and **2** towards ring-opening reactions (vide infra). The NCN signal in **3** also resonates at a similar downfield chemical shift of $\delta = 159.4$ ppm.

Unlike common monodentate NHC ligands bearing bulky *N*-substituents,^[5,6] the monodentate carbene ligands derived from **1** and **2** contain amido functionalities that display apparent tolerance under the catalytic conditions (vide infra), demonstrating the potential modifications of the NHC ligands for catalyst immobilization on solid support or nanoparticles.^[34,35] The carbene ligand derived from **3** contains a

picoyl functionality that we hoped to utilize for trapping the decomposed product by metal coordination (*vide infra*).

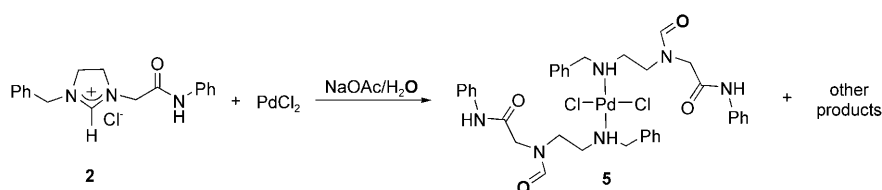
Heterocyclic ring-opened products and their palladium complexes: As shown in Scheme 2, palladium complexes **4** (*cis* and *trans*) have been prepared by us from the ligand precursor



Scheme 2.

precursor **1**.^[15] Under the same reaction conditions with K_2CO_3 in routinely dried DMF, we hoped to prepare analogous palladium complexes **4A** from **2**. However, unlike the reaction between **1** and PdCl_2 that cleanly affords *cis*- and *trans*-**4**, the corresponding reaction gave a complex mixture of products. The messy ^1H NMR spectrum of the mixture, featuring complex signals in the aliphatic region of $\delta = 2.2\text{--}4.8$ ppm indicates the occurrence of ligand degradation. Efforts were made to seek suitable complexation conditions by using different bases and solvents. Upon using sodium acetate as the base in wet acetonitrile, a solid that gave a relatively cleaner ^1H NMR spectrum was obtained (Scheme 3). The spectrum consisted of a downfield signal at approximately $\delta = 10.0$ ppm and a broad signal at approximately $\delta = 4.9$ ppm. A small amount of crystals were successfully prepared and after subsequent structural determination, these signals can be assigned to the aldehyde and amine protons, respectively.

The structure of compound **5** was revealed by X-ray crystallography (Table 1, Figure 1). Pd1 is in a square-planar coordination environment with two *trans* organic ligands and two *trans* chloride ligands. The organic ligands are bound to the metal through secondary-amine moieties. The *N*-formyl group present on the ligand indicates that it is a ring-opened product of the imidazolium salt **2**. No such ring-opened



Scheme 3.

product or its palladium complex were ever observed with the imidazolium salt **1**.^[15]

To explain the ring-opening reaction leading to the formation of **5**, two possible pathways were proposed (Scheme 4). For pathway A, the residual moisture in the solvent can react with sodium acetate to generate hydroxide ions. Since the C2 carbon atom in **2** is quite electrophilic as revealed by its downfield ^{13}C resonance (*vide supra*), it can be attacked readily by the hydroxide ion leading to a mixture of ring-opened products. The ring-opened product **B** was eventually trapped by PdCl_2 to form **5**. In contrast, the imidazolium salt **1** is less vulnerable to such a reaction because its corresponding C2 carbon atom is much less electrophilic as indicated by its more upfield spectroscopic resonance. Conse-

Table 1. Crystallographic data for compounds **5** and **6**.

Compound	5	6
empirical formula	$\text{C}_{30}\text{H}_{42}\text{Cl}_2\text{N}_6\text{O}_4\text{Pd}$	$\text{C}_{16}\text{H}_{19}\text{Cl}_2\text{N}_5\text{OPd}$
F_w	800.06	446.64
crystal system	orthorhombic	monoclinic
space group	$Pna2_1$	$P2_1/c$
a [Å]	19.9958(7)	8.0280(5)
b [Å]	8.2203(3)	8.5842(5)
c [Å]	22.2150(8)	24.7086(16)
α [°]	90	90
β [°]	90	96.797(3)
γ [°]	90	90
V [Å ³]	3651.5(2)	1690.80(18)
D_c [mgm ⁻³]	1.455	1.755
T [K]	150(2)	150(2)
Z	4	4
no. of unique data	9418	3499
no. of parameters refined	443	208
R_1 ^[a] [$I > 2\sigma I$]	0.0440	0.0458
wR_2 ^[b] (all data)	0.0900	0.0987

[a] $R_1 = \sum(|F_o| - |F_c|) / \sum |F_o|$. [b] $wR_2 = [\sum(|F_o|^2 - |F_c|^2)^2 / \sum(F_o^2)]^{1/2}$.

quently, instead of nucleophilic attack, the acidic proton on the C2 carbon atom will be deprotonated, leading to a carbene species that is then trapped by PdCl_2 to form the palladium carbene complex **4**.^[15] For pathway B, the proton on the C2 carbon atom was initially deprotonated by base. The transient carbene species was, however, reacted with water and subsequently formed the ring-opened product **B**. In contrast, the reaction of the carbene derived from **1** with water is less favorable. The contrasting activities displayed between the saturated and un-

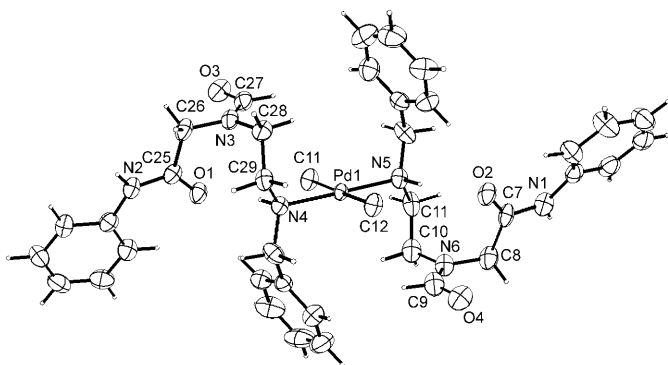
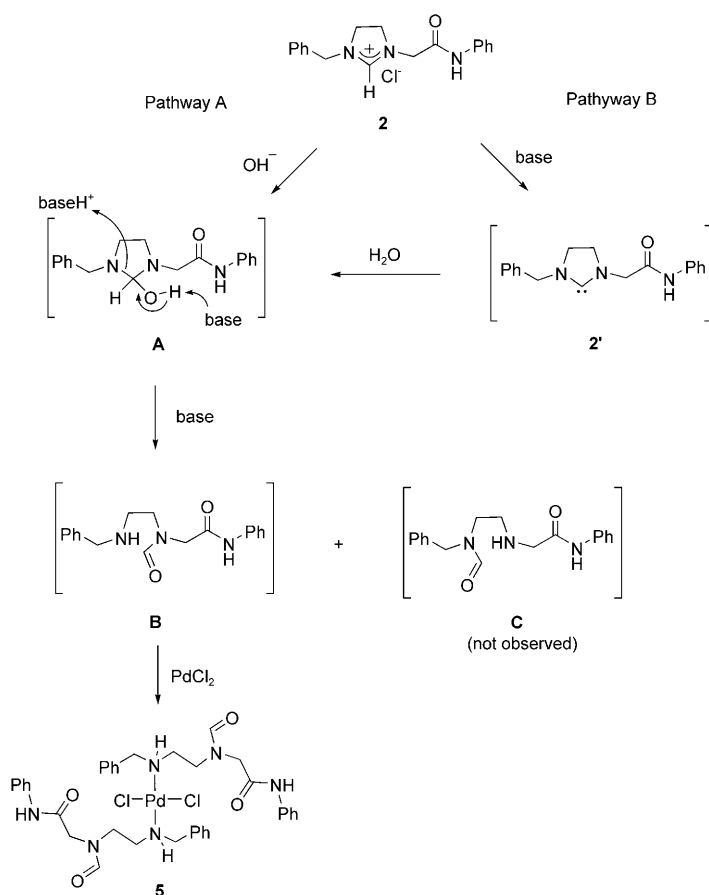


Figure 1. Molecular structure of complex **5**. Thermal ellipsoids are given at the 50% probability level. Selected bond distances [Å]: Pd1–Cl1, 2.2975(10); Pd1–Cl2, 2.3007(10); Pd1–N4, 2.057(3); Pd1–N5, 2.056(3); selected bond angles [°]: N4–Pd1–Cl1, 88.69(10); N4–Pd1–Cl2, 91.10(10); N5–Pd1–Cl2, 89.63(10); N5–Pd1–Cl1, 90.58(10); N4–Pd1–N5, 179.26(15); Cl1–Pd1–Cl2, 179.58(5).



Scheme 4.

saturated compounds is fully supported by our theoretical calculations (vide infra).

In fact, the opening of the imidazole ring forming the *N*-formyl product is a common phenomenon in biological processes,^[36–39] such as DNA damage. Even though NHCs based on the imidazolin-2-ylidene moiety are commonly employed ligands, reports on their hydrolysis are lacking.^[40] Denk

et al. has structurally characterized a relevant ring-opened product, *N*-formyl-*N,N*-di-*tert*-butylethylenediamine from 1,3-di-*tert*-butylimidazolin-2-ylidene.^[40] Ring-opening reactions of NHCs has also been observed by Grubbs et al. on a saturated carbene nickel complex.^[41] The cleavage is, however, carried out by means of an intramolecular attack by a phenyl group on the coordinated carbene.

Since only a low yield of **5** among other ring-opened products was obtained from **2**, we decided to investigate a related ring-opening reaction by using the imidazolium salt **3**. Our hope is based on the coordination ability of the pyridine group in **3**, such that after decomposition, stable chelate complexes of palladium can be obtained and, hence, a higher yield of a single ring-opened product favored. Under similar complexation conditions, however, we obtained a mixture of products according to ¹H NMR spectroscopy. Attempts to separate the mixture were unsuccessful. However, small amounts of crystals were also successfully obtained out of this mixture. Structural analysis confirmed that the compound formed, **6**, is a palladium complex featuring a ring-opened product from **3** (Figure 2). Unlike **5**, the ligand is, as anticipated, chelated in a bidentate fashion by the secondary amine and pyridyl functionalities.

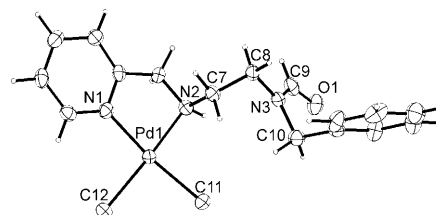
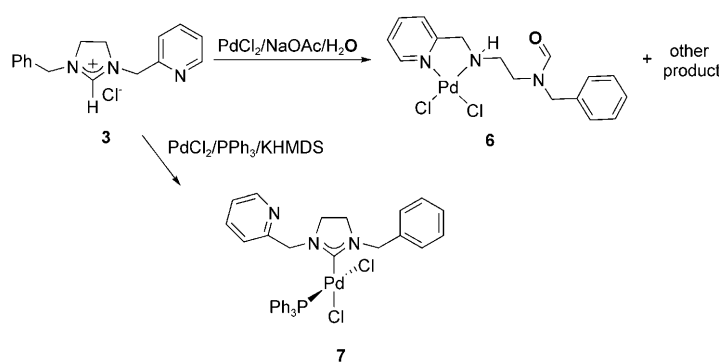


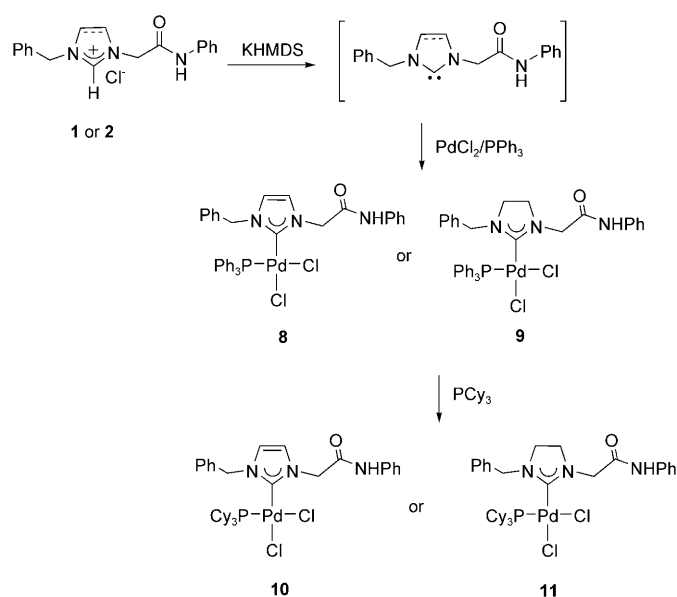
Figure 2. Molecular structure of complex **6**. Thermal ellipsoids are given at the 50% probability level. Selected bond distances [Å]: Pd1–N1, 2.020(4); Pd1–N2, 2.032(4); Pd1–Cl1, 2.2903(14); Pd1–Cl2, 2.2984(13); selected bond angles [°]: N1–Pd1–Cl2, 94.53(12); N1–Pd1–N2, 82.15(17); Cl1–Pd1–Cl2, 92.49(5); Cl1–Pd1–N2, 90.84(12); N1–Pd1–Cl1, 172.97(12); N2–Pd1–Cl2, 175.35(12).

Preparation of mixed phosphine/carbene palladium complexes:

Due to the difficulty in obtaining complex **4A** for comparative studies with complex **4** (Scheme 2), we explored several conditions and found that mixed phosphine/carbene palladium complexes featuring different combinations of NHC ligands (saturated vs. unsaturated) and phosphine ligands (PPh₃ vs. PCy₃) can be obtained in a much easier fashion. Amid low yields, treatment of imidazolium and imidazolium salts **1–3** with PdCl₂ in the presence of potassium hexamethyldisilazane (KHMDs)^[42] and PPh₃ in acetonitrile allowed us to obtain pure mixed *cis* PPh₃/carbene palladium complexes **8**, **9**, and **7**, respectively, (Schemes 5 and 6). The use of the sterically hindered strong base KHMDs in the generation of NHCs has been documented.^[43–45] The new complexes are air and moisture stable and poorly dissolve in common organic solvents. All the NMR spectra of **7–9** contain sharp signals. The successful



Scheme 5.



Scheme 6.

formation of **7–9** is indicated by the disappearance of the signal due to the proton upon the C2 carbon atom and the downfield coordination shift of the PPh₃ signal (for example, from ca. $\delta = -6$ ppm in the free ligand to ca. $\delta = 28$ ppm in **7**). The downfield NH signals at approximately $\delta = 10–11$ ppm in **8** and **9** indicate that the ligands are coordinated in a monodentate fashion. Intriguingly, the carbene carbon atom signals in **7** and **9** resonate at approximately $\delta = 190$ ppm, that is very downfield relative to those of unsaturated carbene palladium complexes. The carbene carbon atom in **8** with the unsaturated NHC resonates $\delta = 30$ ppm more upfield at $\delta = 160$ ppm (vide infra) and in the *trans*-pyridine dichloride palladium complex with the same unsaturated ligand $\delta = 39$ ppm more upfield at approximately $\delta = 151$ ppm.^[15] Similar to the situation of the ligand precursors described above, the more downfield carbene carbon atom in saturated carbene complexes indicates that the carbene carbon atom is much more electrophilic, such that intramolecular nucleophilic attack might occur readily.^[41] Noticeably, these carbene signals are all singlets; the zero ²J coupling constants strongly indicate that they are *cis* com-

plexes, which was confirmed subsequently by X-ray structural studies.

The PCy₃/carbene palladium complexes **10** and **11** were readily prepared by ligand substitution reactions with **8** and **9** by PCy₃, respectively. All the NMR spectroscopic signals are also sharp. The successful formation of **10** and **11** was clearly indicated by the downfield shift of the ³¹P NMR spectroscopic signals. For example, the ³¹P NMR signal shifts from $\delta = 27.6$ in **9** to 49.4 ppm in **11**. Similar to their parent compounds, the carbene resonances are all singlets, which also implies the formation of *cis* complexes. The carbene carbon atom in **10** resonates at $\delta = 164.1$ ppm, whereas that in **11** resonates $\delta = 30$ ppm more downfield at 194.1 ppm. Both complexes exhibit poor solubility in common organic solvents. The solubility of **10** in polar solvents is slightly better than that of **11**.

The behavior of **8–11** in solution is in sharp contrast to that of [PdI₂(NHC)(PR₃)], which exhibits a *cis/trans* isomerization in solution.^[30] They appear to be rigid in solution as only sharp signals are observed in all their spectra and signal broadening is not observed according to a variable-temperature NMR spectroscopic study. Subsequent DFT calculations indicated that these compounds are *cis* isomers in polar solvents (vide infra). All ¹H and ¹³C{¹H} NMR spectroscopic assignments of the complexes have been confirmed by HMBC spectra (see the Supporting Information for an example).

Structural analyses of mixed phosphine/carbene palladium complexes: The structures of **7–11** were unambiguously determined by X-ray crystallography (Table 2, Figures 3–7). Each of these complexes contains a monodentate NHC and a phosphine ligand; the palladium center adopts closely a square-planar coordination geometry with the two ligands coordinating in a *cis* fashion. There are several examples of *cis* PPh₃/carbene Pd^{II} complexes in the literature.^[46–49] Examples of *trans* phosphine/carbene Pd⁰[50] and Pd^{II}[50] complexes are also known. However, *cis* PCy₃/carbene Pd^{II} complexes, such as **10** and **11** are unprecedented in the literature. Despite the large differences in the electronic properties between PPh₃ and PCy₃, the Pd–carbene distances in **7–11** span a narrow range of $\delta = 1.960–1.980$ Å. A related *cis* PPh₃/carbene Pd complex has a Pd–carbene distance of 1.981(2) Å.^[46] Notably, the structure **8** contains two independent molecules in an asymmetric unit. The two Pd–carbene distances (1.960(3) and 1.973(2) Å) vary slightly. The Pd–phosphine distances are also in a narrow range (2.258–2.269 Å) with the Pd–PPh₃ bonds in **8** and **9** slightly shorter than the Pd–PCy₃ bonds in **10** and **11**. Except in **7**, the Pd–Cl bonds *trans* to the phosphine atoms are generally longer than those *trans* to the carbene moieties, which indicates the higher *trans* influence exerted by the phosphine relative to the carbene groups in **8–11**. This is surprising for **8** and **9** since PPh₃ is believed to be a weaker donor than NHC.

The steric effect of phosphine ligands (PCy₃ vs. PPh₃) on the *cis* coordination of the carbene ligands are carefully examined. As expected, the steric bulk of PPh₃ in **7–8** imposes

Table 2. Crystallographic data for compounds **7–11**.

Compound	7	8	9	10	11
empirical formula	C ₃₄ H ₃₂ Cl ₂ N ₃ PPd	C ₃₆ H ₃₂ Cl ₂ N ₃ OP Pd	C ₃₆ H ₃₄ Cl ₂ N ₃ OPPd·CHCl ₃	C ₃₆ H ₃₀ Cl ₂ N ₃ OPPd	C ₃₆ H ₅₂ Cl ₂ N ₃ OPPd
<i>F</i> _w	690.90	730.92	852.30	749.06	751.08
crystal system	monoclinic	triclinic	triclinic	triclinic	triclinic
space group	<i>P</i> 2 ₁ / <i>n</i>	<i>P</i> 1̄	<i>P</i> 1̄	<i>P</i> 1̄	<i>P</i> 1̄
<i>a</i> [Å]	11.5605(10)	9.3137(7)	9.6182(3)	9.6321(4)	9.4734(6)
<i>b</i> [Å]	18.4609(16)	13.7827(11)	13.3049(5)	14.0027(5)	14.0152(8)
<i>c</i> [Å]	14.9203(13)	25.6578(19)	15.0616(5)	14.3449(6)	14.4231(9)
<i>α</i> [°]	90	79.7670(10)	76.470(2)	98.303(2)	97.930(2)
<i>β</i> [°]	104.207(2)	84.039(2)	82.146(2)	107.497(2)	107.519(2)
<i>γ</i> [°]	90	84.7470(10)	85.054(2)	104.217(2)	103.743(2)
<i>V</i> [Å ³]	3086.9(5)	3214.7(4)	1853.41(11)	1738.19(12)	1727.92(18)
<i>D</i> _c [mgm ⁻³]	1.487	1.510	1.527	1.431	1.444
<i>T</i> [K]	150(2)	150(2)	150(2)	150(2)	150(2)
<i>Z</i>	4	4	2	2	2
no. of unique data	7970	16604	9477	10047	8848
no. of parameters refined	379	793	481	425	397
<i>R</i> ₁ ^[a] [<i>I</i> > 2σ <i>I</i>]	0.0442	0.0365	0.0502	0.0434	0.0322
<i>wR</i> ₂ ^[b] (all data)	0.1145	0.0786	0.1142	0.0986	0.0832

[a] $R_1 = \Sigma(|F_o| - |F_c|) / \Sigma |F_o|$. [b] $wR_2 = [\Sigma(|F_o|^2 - |F_c|^2)^2 / \Sigma(F_o^2)]^{1/2}$.

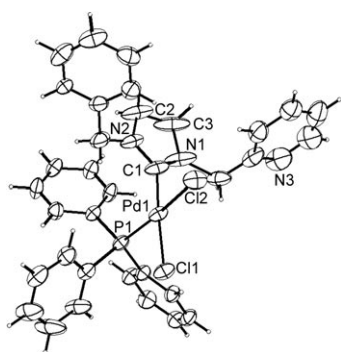


Figure 3. Molecular structure of complex **7**. Thermal ellipsoids are given at the 50% probability level. The picolyl group is disordered with two different orientations. Only the major orientation (occupancy factor = 64%) is shown. Selected bond distances [Å]: Pd1–C1, 1.977(4); Pd1–P1, 2.2625(9); Pd1–C11, 2.3649(8); Pd1–Cl2, 2.3504(9); C2–C3, 1.491(8); selected bond angles [°]: C1–Pd1–P1, 91.72(10); C1–Pd1–Cl2, 86.79(10); P1–Pd1–C11, 89.82(3); C11–Pd1–Cl2, 91.91(3); C1–Pd1–C11, 176.39(13); P1–Pd1–Cl2, 175.53(4).

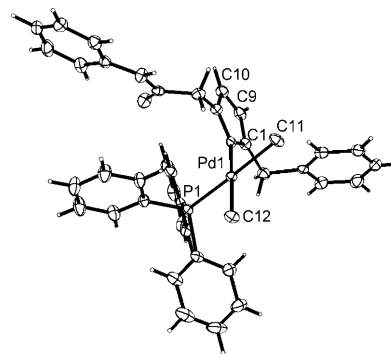


Figure 4. Molecular structure of complex **8**. Thermal ellipsoids are given at the 50% probability level. Only one of the independent molecules in an asymmetric unit is shown (the other molecule is shown in the Supporting Information). Selected bond distances [Å]: Pd1–C1, 1.973(2); Pd1–P1, 2.2572(6); Pd1–C11, 2.3583(6); Pd1–Cl2, 2.3459(6); C9–C10, 1.344(3); selected bond angles [°]: C1–Pd1–P1, 92.59(7); C1–Pd1–C11, 87.03(7); P1–Pd1–Cl2, 89.68(2); C11–Pd1–Cl2, 90.60(2); C1–Pd1–Cl2, 176.41(7); P1–Pd1–C11, 177.92(2).

no significant steric hindrance on the adjacent NHC ligands as suggested by the \angle C–Pd–P angles being close to the ideal 90°. The angles are 91.72(10) in **7**, 92.59(7) and 90.21(7) in **8**, and 93.65° in **9**. Contrastingly, a large steric hindrance imposed by the *cis* disposition of the bulky PCy₃ ligand and the NHC ligand exists in **10** and **11**. There is a pronounced expansion of \angle C–Pd–P from the ideal 90 to 98.16(6)° in **11**. The structure of **10** is isomorphous to that of **11**. Unlike the structure of **11**, there are two orientations for the disordered imidazole ring in **10**. The site for C10 is shared between the two orientations. The \angle C–Pd–P of 97.42(9)° in **10** is similar to that in **11**, which indicates a similar level of steric crowding between the carbene and the PCy₃ ligands. But the two different possible orientations for the unsaturated ring in **10** suggests a higher degree of freedom for the ligand, which is consistent with the smaller steric bulkiness of the unsaturated relative to the saturated carbene.^[19] The effect of the

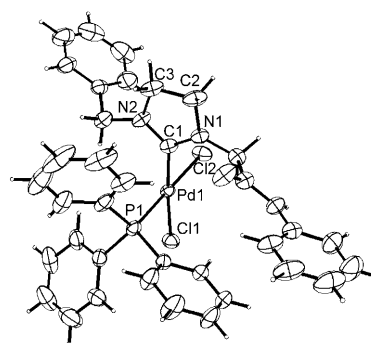


Figure 5. Molecular structure of complex **9**. Thermal ellipsoids are given at the 50% probability level. Selected bond distances [Å]: Pd1–C1, 1.980(4); Pd1–P1, 2.2577(10); Pd1–C11, 2.3357(10); Pd1–Cl2, 2.3526(10); C2–C3, 1.523(6); selected bond angles [°]: C1–Pd1–P1, 93.65(10); C1–Pd1–Cl2, 83.36(10); P1–Pd1–C11, 89.49(4); C11–Pd1–Cl2, 90.49(3); C1–Pd1–C11, 175.83(11); P1–Pd1–Cl2, 179.79(4).

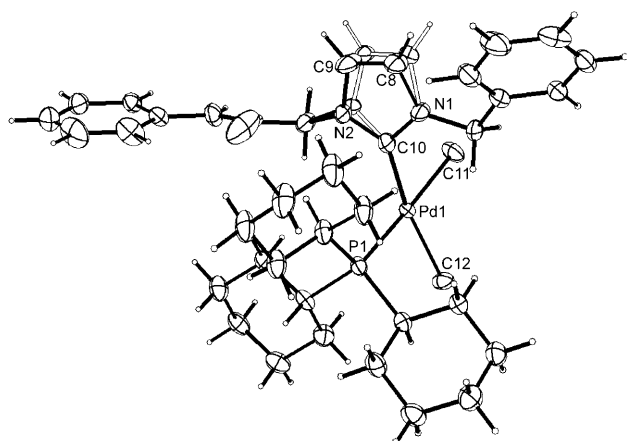


Figure 6. Molecular structure of complex **10** showing two orientations of the imidazole ring. Thermal ellipsoids are given at the 50% probability level. Selected bond distances [Å]: Pd1–C10, 1.976(3); Pd1–P1, 2.2692(7); Pd1–Cl1, 2.3691(7); Pd1–Cl2, 2.3532(7); C8–C9, 1.336(8); selected bond angles [°]: C10–Pd1–P1, 97.42(9); P1–Pd1–Cl2, 91.08(2); C10–Pd1–Cl1, 80.88(10); Cl1–Pd1–Cl2, 90.73(3); C10–Pd1–Cl2, 170.80(9); P1–Pd1–Cl1, 177.64(3).

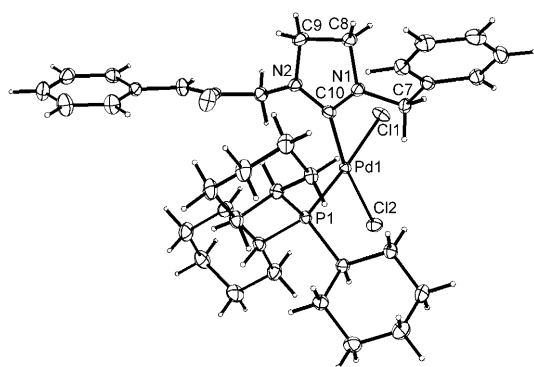
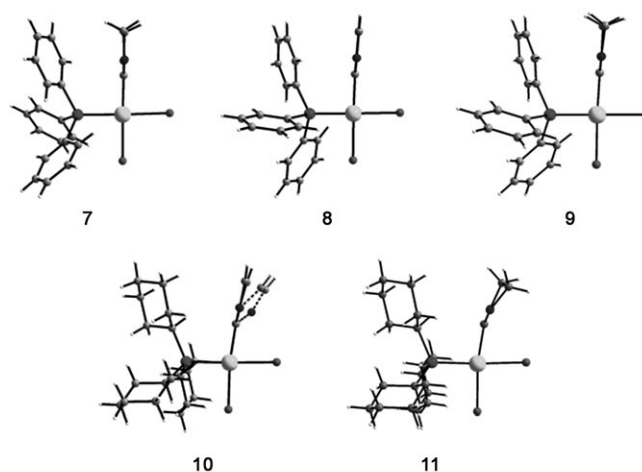


Figure 7. Molecular structure of complex **11**. Thermal ellipsoids are given at the 50% probability level. Selected bond distances [Å]: Pd1–C10, 1.975(2); Pd1–P1, 2.2671(6); Pd1–Cl1, 2.3737(5); Pd1–Cl2, 2.3620(6); C8–C9, 1.511(3); selected bond angles [°]: C10–Pd1–P1, 98.16(6); P1–Pd1–Cl2, 91.24(2); C10–Pd1–Cl1, 79.10(6); Cl1–Pd1–Cl2, 91.65(2); C10–Pd1–Cl2, 169.92(6); P1–Pd1–Cl1, 176.32(2).

steric bulkiness from the *cis* site on the carbene coordination in **7–11** can be collectively visualized in Figure 8. It clearly illustrates the flexibility of the carbene ligands in accommodating the steric change around the Pd center. With the bulky PCy₃ ligand, the NHC ligands are tilted significantly to release the steric strain. Because of the steric hindrance in **10** and **11**, it is quite surprising that the *cis* instead of the *trans* complexes are prevailing. Another noticeable feature is the puckering of the saturated ring in **11**, whereas the rings in **7** and **9** are more planar; the N1–C7–C8–C10 unit in **11** is pyramidal with the N1 atom 0.244(2) Å out of the plane of the three carbon atoms.

Electronic aspect probed by X-ray photoelectron spectroscopy (XPS): Complexes **8–11** feature different combinations of NHC ligands (saturated vs. unsaturated) and phosphine



	compound	∠C–Pd–P
	7	91.72°
	8	92.59°*
	9	93.65°
	10	97.42°
	11	98.16°

* Only one of the independent molecules is shown.

Figure 8. Ball and stick representations of **7** and **9–11** illustrating the severe distortion of the heterocyclic ring in **10** and **11**. The N-substitutions were removed for clarity.

ligands (PPh₃ vs. PCy₃). We tried to probe the donating properties of each set of ligand combinations in **8–11** by X-ray photoelectron spectroscopic studies. Markedly for **8–11**, the binding energies of Pd electrons in the core 3d_{5/2} and 3d_{3/2} orbitals are about 343 and 337 eV, respectively, which are exceptionally low. For comparison, the corresponding binding energies in Pd^{II} complexes with a bidentate carbene of abnormal binding are much higher at approximately 348.0 and 342.6 eV.^[51] In fact, the binding energies for the new Pd^{II} complexes are very close to those of 340.5 and 335.1 eV in Pd⁰.^[52] The low electron binding in **8–11** indicates that their Pd^{II} centers are highly electron-rich due to the very strong electron-donating nature of the phosphine/carbene ligand set. The order of the binding energies for the 3d_{5/2} electron follows the order **8** (336.937 eV) > **9** (336.818 eV) > **10** (336.735 eV) > **11** (336.721 eV) (Figure 9), reflecting that **8** with PPh₃ and the unsaturated NHC ligand is the least electron-rich complex. A comparison of the binding energies in **8** and **9** shows that the saturated NHC is more electron donating than the unsaturated carbene ligand. The difference, however, becomes less pronounced in the electron-rich complexes **10** and **11** containing the strong donating PCy₃ ligand.

Computational studies: There is a higher propensity of **2** to undergo a ring-opening reaction than its unsaturated analogue **1** (Scheme 4). The more electrophilic nature of the C2

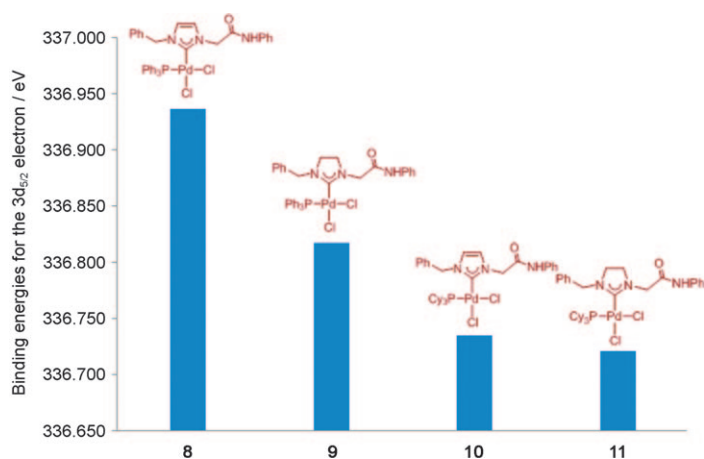
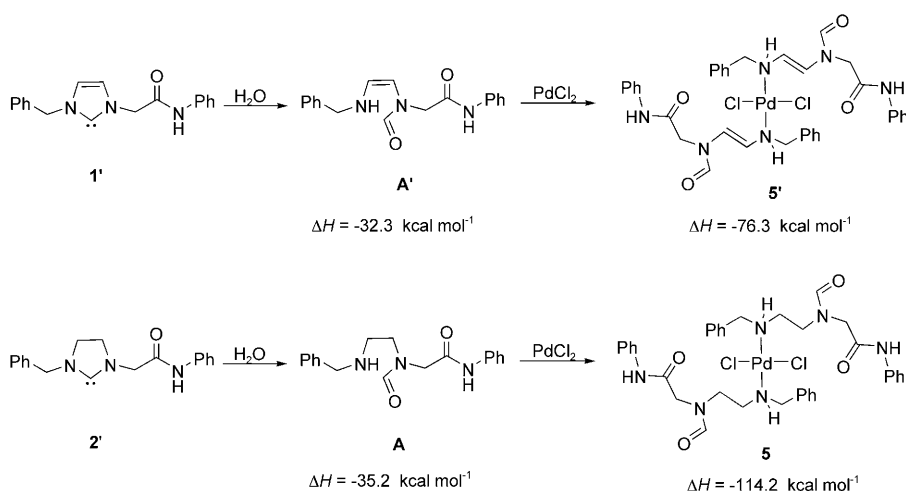


Figure 9. XPS spectra (3d level) of **8–11**.

carbon atom in **2** as indicated by $^{13}\text{C}\{^1\text{H}\}$ NMR spectroscopy may explain the difference. More evidence for this trend was obtained from theoretical calculations. Natural bond-orbital analysis by using the B3LYP method was applied for this purpose. Indeed, the natural charge on the NCN carbon atom of **2** was computed to be 0.352, which is higher than that of 0.266 on **1**. For pathway B, the natural charges on the carbenic carbon atom on **2'** are also higher and about two times that of **1'** (0.170 vs. 0.084), reflecting the higher vulnerability of **2'** to be attacked by H_2O . Moreover, the higher tendency of **2** to undergo ring-opening reactions is clearly reflected from the thermodynamics (Scheme 7). The transient carbene **2'** reacts with H_2O to form **A** with a ΔH of $-35.2 \text{ kcal mol}^{-1}$, that is, approximately $2.9 \text{ kcal mol}^{-1}$ more negative than the corresponding reaction with the carbene **1'**. The difference in the ΔH values becomes even more obvious in the presence of PdCl_2 . The ΔH of $-114.2 \text{ kcal mol}^{-1}$ for the formation of **5** is about 1.5 times that of the corresponding reaction from the unsaturated carbene.



Scheme 7.

Intriguingly, only the *cis* complexes were observed for **7–11**, despite the fact that considerable steric hindrance exists in these isomers, especially for **10** and **11**. Therefore, we sought to determine the relative energies between the *cis* and *trans* isomers by computational studies with the B3LYP functional. In contrast to our experimental findings, the gas-phase computations showed that the *trans* complexes **8'**, **9'**, **10'**, and **11'** (see Figure 3S in the Supporting Information) are more stable than their *cis* counterparts by 0.8, 1.1, 12.6, and $6.1 \text{ kcal mol}^{-1}$, respectively. Since polar solvents (acetonitrile and dichloromethane) were used for the preparation of these compounds, solvent effects may play a vital role in the predominant formation of the *cis* complexes.^[16] The solvation effects might favor the more polar *cis* isomers (the dipole moments of **8**, **9**, **10**, and **11** are 9.98, 10.69, 11.92, and 11.09 D, whereas the corresponding *trans* complexes are only 2.84, 2.39, 4.03, and 1.62 D , respectively). Therefore, the solvation effects of compounds in acetonitrile are included by using the CPCM model.^[53] We found indeed that the *cis* complexes become more stable than their *trans* counterparts by 4.6, 10.4, 4.2, and $7.3 \text{ kcal mol}^{-1}$, respectively.

Even though complex **4A** was not achieved under our experimental conditions, we did a DFT calculation by using the B3LYP density functional to understand the difference between the binding energies of carbenes **1'** and **2'** for the formation of their corresponding bis-chelate complexes. The $-\Delta H$ values for **1'** to form *cis*- and *trans*-**4** are found to be 15.9 and $17.3 \text{ kcal mol}^{-1}$, respectively. Surprisingly, the $-\Delta H$ values for the saturated **2'** to form *cis*- and *trans*-**4A** are approximately 0.3 and $1.1 \text{ kcal mol}^{-1}$ smaller (15.6 and $16.2 \text{ kcal mol}^{-1}$), which indicates that, in contrast to our XPS findings, the unsaturated carbene binds to Pd^{II} even better than the saturated analogue. In fact, it has been reported that the difference in experimental enthalpies between saturated and unsaturated carbenes in metal binding is quite small.^[19] For example, the difference in bond dissociation energies between IMes and SIMes is also approximately $+1 \text{ kcal mol}^{-1}$. In the case of IPr and sIPr, the former ligand binds even better than the saturated analogue.^[19] The lower $-\Delta H$ value for the formation of *cis* complexes can be attributed to steric reasons.

Thermal stability: For catalytic applications, high stability of the precatalyst towards air, moisture, and heat are desirable characteristics. The question as to whether the highly electron-rich compounds **8–11**, especially those containing the electron-rich PCy_3 , are thermally stable or not needs to be addressed. As an illustrative example, a $[\text{D}_7]\text{DMF}$ solution of **10** was prepared in air and a

variable-temperature $^{31}\text{P}\{^1\text{H}\}$ NMR spectroscopic study was performed. On heating up to 80°C , the singlet at $\delta = 46.0$ ppm remained intact with no new peak observed, which indicated the stability of the *cis* complex. This result is in contrast to that reported for $[\text{PdI}_2(\text{NHC})(\text{PR}_3)]$, which exhibits *cis/trans* isomerization exchange and ligand exchange equilibrium as well.^[30] The latter process produced bis(phosphine) palladium and bis(NHC) palladium species in the solution.^[30] In addition, thermal gravimetric analyses (TGA) on solid samples of **8–11** under N_2 were performed, which indicated that all the complexes are highly stable (Figure 10). Their onset temperatures of decomposition are in the range of $272\text{--}300^\circ\text{C}$.

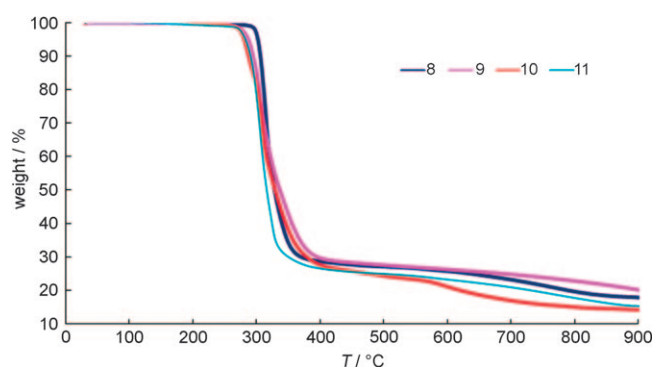


Figure 10. The high thermal stability of **10** displayed by TGA analysis.

Catalytic studies: The palladium(II) complexes were tested in benchmark Suzuki coupling reactions of aryl halides with phenylboronic acid (Table 3). While all complexes deliver

Table 3. Suzuki coupling with aryl chlorides.^[a]

Entry	Cat.	mol%	R	t [h]	Yield [%]
1	8	1	COMe	2	8
2	9	1	COMe	2	4
3	10	1	COMe	2	100
4	11	1	COMe	2	100 (90) ^[b]
5	10	2	Me	0.5	30
		2	Me	1	67
		2	Me	2	78
		2	Me	4	81
		2	Me	6	81
6	11	2	Me	12	82
		2	Me	0.5	56
		2	Me	1	62
		2	Me	2	75
		2	Me	4	77
7	10	2	Me	6	79
		2	Me	12	80
		3	OMe	12	83
8	11	3	OMe	12	79

[a] Reaction conditions: aryl chloride (1 mmol), of $\text{PhB}(\text{OH})_2$ (1.5 mmol), Cs_2CO_3 as base (2.0 mmol), catalyst (1–3 mol%), 1,4-dioxane (3 mL), 80°C , GC yield. [b] Isolated yield.

excellent coupling activities with aryl bromides as substrates, entries 1–4 indicate that only the PCy_3 complexes **10** and **11** can effectively catalyze the reactions with unreactive aryl chlorides as substrates. Quantitative yields of 4-acetobiphenyl can be achieved with a mere 1 mol% catalyst loading in 2 h. Complexes **10** and **11** were also efficient in utilizing unreactive electron-neutral 4-chlorotoluene (entries 5 and 6). A comparison of the time/yield characteristics of **10** and **11** indicates that the unsaturated and saturated carbene complexes deliver the same level of activities (see also Figure S4 in the Supporting Information). Both complexes afford good yields of 4-phenyltoluene (ca. 80%) with a 2 mol% of catalyst loading in approximately 6 h. The two complexes are also effective in delivering good coupling activities with the highly unreactive 4-chloroanisole (entries 7 and 8). Their activities are higher than those reported for $[\text{PdI}_2(\text{NHC})(\text{PR}_3)]$ by Herrmann et al., in which a higher temperature and a longer reaction time were required.^[30] Notably, the dangling *N*-amido functionality on the ligand shows tolerance under the catalytic conditions, which allows future immobilization of catalyst on solid supports.^[54–56]

To probe the possible catalytic species responsible for the activity, we performed catalytic runs in which two equivalents of PR_3 (with respect to the catalyst) were added initially (Table 4). In comparison with the control run (entry 1),

Table 4. The effect of excess PR_3 and Hg^0 on the Suzuki coupling.^[a]

Entry	PR_3 or Hg	mol%	t [h]	Yield [%]
1	–	–	4	75
2	PPh_3	4	4	2 ^[b]
3	PCy_3	4	4	20 ^[b]
4	PPh_3	4	4	60 ^[c]
5	Hg^0	600	4	0 ^[b]
6	Hg^0	600	4	64 ^[c]

[a] Reaction conditions: aryl chloride (1 mmol), $\text{PhB}(\text{OH})_2$ (1.5 mmol), Cs_2CO_3 as base (2.0 mmol), catalyst (2 mol%), PR_3 (0–4 mol%), 1,4-dioxane (3 mL), 80°C , GC yield. [b] Initial addition of PR_3 or Hg^0 . [c] Addition of PR_3 or Hg^0 after 15 min at 80°C .

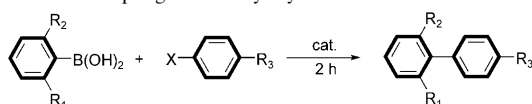
excess PR_3 slowed down the catalytic reactions prominently (entries 2 and 3), which reflects the involvement of phosphine dissociation for the formation of an active homogeneous (NHC)– Pd^0 species.^[4,23,50,57] The higher activities of the PCy_3 /carbene complexes relative to the PPh_3 /carbene complexes can be attributed to the faster de-coordination of the labile PCy_3 ligand and facile formation of Pd^0 species due to the more electron-rich nature of the Pd^{II} centers. After the formation of the active (NHC)– Pd^0 complex, the addition of PPh_3 gives only a slightly lower yield (entry 4).

It is unlikely that the catalytic system involves a heterogeneous nanocluster Pd^0 as the active catalyst.^[58] It has been demonstrated that if less than one equivalent of the added ligand (per metal atom) poisons the catalyst completely, then it is highly suggestive of a heterogeneous catalyst.^[59] Since complex **11** contains one equivalent of PCy_3 , if the

active nanocluster Pd⁰ is formed during the reaction, the dissociated PCy₃ in the vessel should suppress its catalytic activity. Moreover, the mercury test is a facile way to distinguish homogeneous, single-metal-complex catalysts from nanocluster or colloid catalysts.^[59,60] Entry 5 shows that the initial addition of excess Hg⁰ stopped the catalytic reaction, possibly due to the reaction of Hg⁰ with the Pd^{II} complex **11**.^[61] If excess Hg⁰ was added after 15 minutes, allowing the formation of the active species, an overall yield of 64% can still be obtained (entry 6). This result strongly indicates the significant role of a homogenous (NHC)-Pd⁰ complex, rather than a heterogeneous Pd⁰ as the active catalyst.

Complexes **10** and **11** contain the bulky PCy₃ ligand and its dissociation to generate {Pd⁰(NHC)} species should allow coordination of bulky substrates. Therefore, we also tested **8–11** in the coupling activities with sterically demanding 2-methoxyphenylboronic acid and 2,4-methoxyphenylboronic acid (Table 5). In general, excellent yields of mono-*ortho*-substituted biaryl products can be achieved with **8–11** (entries 1–5). With the highly sterically demanding 2,4-methoxyphenylboronic acid as the substrate, a higher catalyst loading of 3 mol% is required to produce a much lower yield of 20% (entries 6).

Table 5. Suzuki coupling with bulky arylboronic acid.^[a]



Entry	Cat.	R ₁	R ₂	R ₃	X	t [h]	Yield [%] ^[a]
1	8	OMe	H	OMe	Br	2	86
2	9	OMe	H	OMe	Br	2	87
3	10	OMe	H	OMe	Br	2	92
4	11	OMe	H	OMe	Br	2	93
5	11	OMe	H	COMe	Cl	12	85
6	11	OMe	OMe	OMe	Br	2	20 ^[b]

[a] Reaction conditions: aryl halides (1 mmol), ArB(OH)₂ (1.5 mmol), Cs₂CO₃ as base (2.0 mmol), catalyst (1 mol%), 1,4-dioxane (3 mL), 80 °C, isolated yield. [b] Catalyst (3 mol%).

For the production of fine chemicals by using palladium-catalyzed reactions, the amount of Pd metal remaining in the biphenyl product is an important concern. The content of Pd⁰ in the products from entry 4 in Table 3 prior to and after purification with column chromatography were 777.5 and 57.16 ppm, respectively, as determined by ICP-MS.

Conclusion

While homoleptic palladium complex **4** was easily obtained, the difficulty to obtain the corresponding saturated carbene analogue **4A** can be related to a facile ring-opening reaction even with a trace amount of moisture. Two palladium complexes with the ring-opened products were structurally characterized. The higher vulnerability of imidazolium salt **2** than imidazolium salt **1** to ring-opening reactions is, as

shown by the theoretical calculations, related to the more electropositive C2 carbon atom in **2** or **2'**, which facilitates the nucleophilic attack by water.

The *cis* phosphine/carbene palladium(II) complexes **8–11** can be easily prepared from **1** and **2**. The XPS study shows that these complexes are highly electron rich. The binding energies of the core 3d electrons are close to that of Pd⁰. Despite the electron-rich nature of these complexes, TGA analysis indicated that they are of high thermal stability (ca. 272–300 °C). As an alternative to the existing systems of [PdCl(allyl)(NHC)]^[18] and [PdCl₂(3-chloropyridine)-(NHC)]^[62] *cis*-[PdCl₂(NHC)(PCy₃)] represents a viable Pd^{II} precatalyst that delivers competent coupling activities. Unreactive aryl halides can be applied as substrates. The higher activities of PCy₃/carbene complexes than the PPh₃/carbene complexes can be attributed to the faster dissociation of labile PCy₃ and the facile formation of an active {Pd⁰(NHC)} species from the more electron-rich Pd^{II} precatalysts. The saturated and unsaturated carbene complexes show no difference in activities. As revealed by structural studies, the carbene ligand derived from **1** and **2** can accommodate steric bulkiness in their vicinity. Correspondingly, **10** and **11** exhibit coupling activities with bulky substrates albeit with inferior yields. Further tuning of the N-substitutions on the carbene ligands is under investigation.

Experimental Section

General: All reactions were performed under a dry nitrogen atmosphere by using standard Schlenk techniques.^[63] All solvents used were purified according to standard procedures. Commercially available chemicals were purchased from Aldrich or Acros. ¹H and ¹³C[¹H] NMR spectra were generally recorded at 300.13 and 75.48 MHz, respectively, on a Bruker AV-300 spectrometer. The ¹³C[¹H] NMR spectrum of **11**, because of its limited solubility, was collected at 150.87 MHz on a Varian Inova 600 spectrometer at the Instrument Center of National Chung Hsing University. ³¹P[¹H] NMR spectra were recorded at 121.49 MHz. Chemical shifts for ¹H and ¹³C spectra were recorded in ppm relative to the residual proton of CDCl₃ (¹H: δ = 7.24, ¹³C: 77.0 ppm), CD₂Cl₂ (¹H: δ = 5.32, ¹³C: 53.8 ppm), and [D₆]DMSO (¹H: δ = 2.50, ¹³C: 39.5 ppm). Elemental analyses, HRMS, and ESMS were performed on a Heraeus CHN-OS-Rapid elemental analyzer, a Finnigan/Thermo Quest MAT 95XL mass spectrometer, and a Finnigan/Thermo TSQ Quantum triple quadrupole mass spectrometer, respectively, at the Instrument Center of the National Chung Hsing University (Taiwan). Inductively coupled plasma-mass spectrometry (ICP-MS) was performed on a Perkin-Elmer SCIEX ELAN 5000 instrument at the Instrument Center of the National Tsing Hua University (Taiwan). GC analyses were performed on a Varian CP3800 GC system with a CP-Sil 5CB fused silica column (length: 30 mm, ID: 0.32 mm, film thickness: 1 μm). The syntheses of imidazolium salt **1** was carried out according to a literature procedure.^[15] X-ray photoelectron spectroscopy was performed on a ESCA PHI 1600 system by using MgK_α radiation (hν = 1253.6 eV) at the National Tsing Hua University. Cyclic voltammograms were recorded on a CHI 611C electrochemical analyzer.

Synthesis of 2: A mixture of 1-benzyl-1*H*-imidazole (2.81 g, 17.8 mmol) and 2-chloro-*N*-phenylacetamide (3.01 g, 17.8 mmol) in THF (40 mL) was refluxed at 75 °C for 2 days. After cooling, the white solid was filtered, washed with THF twice, and then dried under vacuum. Yield: 5.01 g, 86%; m.p. 186 °C; ¹H NMR ([D₆]DMSO): δ = 3.87 (m, 4H; NCH₂CH₂N), 4.53 (s, 2H; CH₂C=O), 4.77 (s, 2H; PhCH₂), 7.08 (t, J = 7.4 Hz, 1H; Ph-*H*), 7.33 (t, J = 7.4 Hz, 2H; Ph-*H*), 7.43–7.48 (m, 5H; Ph-

H), 7.67 (d, $J=7.4$ Hz, 2H; Ph-*H*), 8.88 (s, 1H; NCHN), 10.94 ppm (s, 1H; NH); $^{13}\text{C}\{^1\text{H}\}$ NMR ($[\text{D}_6]\text{DMSO}$): $\delta=48.4$ (CH_2), 49.8 (CH_2), 50.4 (CH_2), 51.1 (CH_2), 119.6 (CH), 124.1 (CH), 128.9 (CH), 129.2 (CH), 129.3 (CH), 134.2 (CH_2C), 139.0 (O=CNC), 160.0 (NCHN), 165.2 ppm (C=O); positive mode ESMS m/z : 294.23 [$M-\text{Cl}$] $^+$; elemental analysis calcd (%) for $\text{C}_{18}\text{H}_{20}\text{N}_3\text{OCl}$: C 65.55, H 6.11, N 12.74; found: C 65.39, H 6.03, N 12.87.

Synthesis of 3: A mixture of 2-(4,5-dihydro-1*H*-imidazol-1-yl)methylpyridine (2.41 g, 14.9 mmol) and benzyl chloride (1.72 mL, 14.9 mmol) in DMF (8 mL) was allowed to react at 80 °C for 2 days. After cooling, the solvent was completely removed under vacuum. The brown residue was washed several times with THF and diethyl ether, filtered on a frit under nitrogen, and dried under vacuum. The compound is highly hygroscopic. Yield: 3.12 g, 72%; ^1H NMR (CDCl_3): $\delta=3.80$ (m, 4H; $\text{NCH}_2\text{CH}_2\text{N}$), 4.80 (s, 2H; $\text{CH}_2\text{C}=\text{O}$), 4.93 (s, 2H; Ph CH_2), 7.17 (dd, $J=7.5$, 5.1 Hz, 1H; py-*H*), 7.24–7.35 (m, 5H; Ph-*H*), 7.45 (d, $J=7.4$ Hz, 1H; py-*H*), 7.63 (t, $J=7.7$ Hz, 1H; py-*H*), 8.44 (d, $J=4.2$ Hz; py-*H*), 10.34 ppm (s, 1H; NCHN); $^{13}\text{C}\{^1\text{H}\}$ NMR (CDCl_3): $\delta=47.6$ (CH_2), 48.4 (CH_2), 52.0 (CH_2), 52.5 (CH_2), 123.2 (py-CH), 123.3 (py-CH), 128.6 (Ph-CH), 128.7 (Ph-CH), 129.0 (Ph-CH), 132.4 (Ph-C), 137.3 (py-CH), 149.4 (py-CH), 152.6 (py-C), 159.4 ppm (NCHN); positive mode ESMS m/z : 252.15 [$M-\text{Cl}$] $^+$, 270.14 [$M-\text{Cl}+\text{H}_2\text{O}$] $^+$; HRMS (FAB $^+$): calcd for $\text{C}_{16}\text{H}_{18}\text{N}_3$: 252.1501; found: 252.1498.

Synthesis of 5: A mixture of **2** (0.164 g, 0.353 mmol), NaOAc (0.0289 g, 0.353 mmol), and PdCl_2 (0.0313 g, 0.176 mmol) in acetonitrile (initial water content ca. 1–2%; 15 mL) was allowed to react at room temperature for 1 day. The yellow precipitate was collected on a frit, washed with CH_3CN and methanol, and then dried under vacuum. Crystals suitable for X-ray diffraction studies were grown by vapor diffusion of diethyl ether into a 1:1 DMF/MeOH solution of the compound. Yield: 0.0167 g, 12%; m.p. 210 °C (dec).

Synthesis of 6: A mixture of **3** (0.0559 g, 0.309 mmol), NaOAc (0.0253 g, 0.309 mmol), and PdCl_2 (0.0548 g, 0.309 mmol) in CH_3CN (10 mL) was allowed to react at room temperature overnight. The solution was decanted and the residual solid was washed with wet methanol twice. The solid was then filtered under nitrogen and dried under vacuum. The ^1H NMR spectrum indicates a mixture of products. Small amounts of crystals of **6** can be obtained by vapor diffusion of diethyl ether into a DMF solution containing the mixture.

Synthesis of 7: A mixture **3** (0.129 g, 0.488 mmol), KHMDs (0.109 g, 0.448 mmol), PdCl_2 (0.079 g, 0.448 mmol), and PPh_3 (0.1176 g, 0.448 mmol) in acetonitrile (20 mL) was stirred at room temperature overnight. The solution was filtered through a plug of Celite. The solvent was then removed under vacuum. The residue was re-dissolved in THF (20 mL) and the solution was filtered through a plug of Celite. The solvent was reduced to approximately 3 mL. Upon the addition of diethyl ether, a pale-yellow precipitate was formed. The solid was filtered on a frit, washed with diethyl ether and toluene, and dried under vacuum. Crystals suitable for X-ray diffraction studies were grown by vapor diffusion of diethyl ether into a MeOH solution of the compound. Yield: 0.053 g, 17%; m.p. 227 °C; ^1H NMR (CDCl_3): $\delta=2.80$ (virtual q, $J=10.0$ Hz, 1H; $\text{NCH}_2\text{H}_b\text{CH}_c\text{H}_d\text{N}$), 3.09 (virtual q, $J=10.0$ Hz, 1H; $\text{NCH}_2\text{H}_b\text{CH}_c\text{H}_d\text{N}$), 3.26 (m, 2H; $\text{NCH}_2\text{H}_b\text{CH}_c\text{H}_d\text{N}$), 3.68 (d, $J=14.0$ Hz, 1H; $\text{NCH}_2\text{H}_b\text{Ph}$), 4.69 (d, $J=15.0$ Hz, 1H; $\text{NCH}_2\text{H}_b\text{Py}$), 5.39 (d, $J=14.0$ Hz, 1H; $\text{NCH}_2\text{H}_b\text{Ph}$), 5.50 (d, $J=15.0$ Hz, 1H; $\text{NCH}_2\text{H}_b\text{Py}$), 7.04–7.76 (m, 22H; py-*H*, PPh-*H*, Ph-*H*), 7.89 (d, $J=7.8$ Hz, 1H; py-*H*), 8.48 ppm (d, $J=4.2$ Hz, 1H; py-*H*); $^{13}\text{C}\{^1\text{H}\}$ NMR (CDCl_3): $\delta=47.8$ ($\text{NCH}_2\text{CH}_2\text{N}$), 48.9 ($\text{NCH}_2\text{CH}_2\text{N}$), 54.2 (CH_2Ph), 55.8 (CH_2Py), 123.5 (py-CH), 124.4 (py-CH), 128.5–128.8 (PPh-CH, PPh-C, Ph-CH), 129.1 (Ph-CH), 129.8 (Ph-CH), 131.6 (unresolved d; PPh-C), 133.8 (Ph-C), 134.4 (d, $^2J_{\text{PC}}=11.2$ Hz; PPh-CH), 138.0 (py-CH), 149.6 (py-CH), 154.4 (py-C), 192.6 ppm (NCN); $^{31}\text{P}\{^1\text{H}\}$ NMR (121.49 MHz, CDCl_3): $\delta=27.8$ ppm; elemental analysis calcd (%) for $\text{C}_{34}\text{H}_{32}\text{Cl}_2\text{N}_3\text{PPd}$: C 59.10, H 4.67, N 6.08; found: C 59.20, H 4.75, N 6.01.

Synthesis of 8: A mixture of **1** (0.172 g, 0.530 mmol), KHMDs (0.105 g, 0.530 mmol), PdCl_2 (0.0931 g, 0.530 mmol), and PPh_3 (0.138 g, 0.530 mmol) in acetonitrile (20 mL) was allowed to react at room temperature overnight. The precipitate was then collected on a frit, washed with

CH_3CN (10 mL), THF (15 \times 4 mL), and $\text{H}_2\text{O}/\text{MeOH}$ (1:1), and then dried under vacuum. Crystals suitable for X-ray diffraction studies were grown by layer diffusion of dichloromethane into a dichloromethane solution of the compound. Yield: 0.120, 31%; m.p. 298 °C (dec); ^1H NMR ($[\text{D}_6]\text{DMSO}$): $\delta=3.78$ (d, $J=14.4$ Hz, 1H; $\text{NCH}_2\text{H}_b\text{C}=\text{O}$), 5.00 (d, $J=17.0$ Hz, 1H; $\text{NCH}_2\text{H}_b\text{Ph}$), 5.47 (d, $J=14.4$ Hz, 1H; $\text{NCH}_2\text{H}_b\text{C}=\text{O}$), 5.74 (d, $J=17.0$ Hz, 1H; $\text{NCH}_2\text{H}_b\text{Ph}$), 6.82 (d, $J=1.8$ Hz, 1H; imi-*H*), 7.07 (t, $J=7.1$ Hz; Ph-*H*), 7.26–7.53 (t, 25H; Ph-*H*, imi-*H*), 10.35 ppm (s, 1H; NH); $^{13}\text{C}\{^1\text{H}\}$ NMR ($[\text{D}_6]\text{DMSO}$): $\delta=53.2$ (CH_2), 53.5 (CH_2), 119.6 (CH), 121.8 (CH), 123.8 (CH), 126.2 (CH), 128.6 (CH), 128.8 (CH), 128.9–129.4 (overlapping signals CH), 128.8 (CH), 129.4 (CH), 130.2 (CH), 131.4 (unresolved, PC), 134.3 (d, $^2J_{\text{PC}}=11.1$ Hz; PPh-CH), 135.8 (CH_2C), 138.8 (O=CNC), 160.1 (NCN), 164.8 ppm (C=O); $^{31}\text{P}\{^1\text{H}\}$ NMR ($[\text{D}_6]\text{DMSO}$): $\delta=28.0$ ppm; elemental analysis calcd (%) for $\text{C}_{36}\text{H}_{32}\text{Cl}_2\text{N}_3\text{OPPd}$: C 58.46, H 4.67, N 5.56; found: C 58.53, H 4.92, N 5.69.

Synthesis of 9: A mixture of **2** (0.269 g, 0.814 mmol), KHMDs (0.162 g, 0.814 mmol), PdCl_2 (0.144 g, 0.814 mmol), and PPh_3 (0.214 g, 0.814 mmol) was stirred in acetonitrile (25 mL) at room temperature for 1 day. The insoluble solid was collected on a frit, washed with acetonitrile (10 mL) and THF (15 mL \times 4). The solid was then extracted with dichloromethane (50 mL). The solvent was reduced to ca. 3 mL under vacuum. Upon addition of diethyl ether, a white solid was formed. Crystals suitable for X-ray diffraction studies were grown by slow evaporation from its chloroform solution. Yield: 0.15, 26%; m.p. 268 °C (dec); ^1H NMR (CDCl_3): $\delta=2.80$ (virtual q, $J=9.7$ Hz, 1H; $\text{NCH}_2\text{H}_b\text{CH}_c\text{H}_d\text{N}$), 2.96 (virtual q, $J=9.7$ Hz, 1H; $\text{NCH}_2\text{H}_b\text{CH}_c\text{H}_d\text{N}$), 3.18 (virtual q, $J=9.7$ Hz, 1H; $\text{NCH}_2\text{H}_b\text{CH}_c\text{H}_d\text{N}$), 3.39 (virtual q, $J=9.7$ Hz, 1H; $\text{NCH}_2\text{H}_b\text{CH}_c\text{H}_d\text{N}$), 3.45 (d, $J=15.0$ Hz, 1H; $\text{NCH}_2\text{H}_b\text{C}=\text{O}$), 4.08 (d, $J=14.0$ Hz, 1H; $\text{NCH}_2\text{H}_b\text{Ph}$), 5.45 (d, $J=15.0$ Hz, 1H; $\text{NCH}_2\text{H}_b\text{C}=\text{O}$), 5.55 (d, $J=14.0$ Hz, 1H; $\text{NCH}_2\text{H}_b\text{Ph}$), 7.06 (t, $J=7.8$ Hz, 1H; Ph-*H*), 7.23–7.29 (m, 7H; Ph-*H*), 7.42–7.52 (m, 9H; Ph-*H*), 7.68–7.80 (m, 8H; Ph-*H*), 9.74 ppm (s, 1H; NH); $^{13}\text{C}\{^1\text{H}\}$ NMR (CD_2Cl_2): $\delta=47.9$ ($\text{NCH}_2\text{CH}_2\text{N}$), 48.1 ($\text{NCH}_2\text{CH}_2\text{N}$), 54.5 (Ph CH_2), 55.8 (CH_2CO), 119.9 (CH), 124.2 (CH), 128.5 (CH), 128.6 (d, $^3J_{\text{PC}}=2.1$ Hz, PPh-CH), 128.8 (CH), 129.1 (CH), 129.8 (CH), 131.7 (d, $^1J_{\text{PC}}=2.6$ Hz; PC), 133.5 (CH_2C), 134.3 (d, $^2J_{\text{PC}}=11.0$ Hz; PPh-CH), 138.2 (O=CNC), 164.9 (C=O), 193.3 ppm (NCN); $^{31}\text{P}\{^1\text{H}\}$ NMR (CDCl_3): $\delta=27.6$ ppm; elemental analysis calcd (%) for $\text{C}_{36}\text{H}_{34}\text{Cl}_2\text{N}_3\text{OPPd}$: C 58.99, H 4.67, N 5.73; found: C 58.79, H 4.75, N 5.63.

Synthesis of 10: A mixture of **8** (0.105 g, 0.143 mmol) and PCy_3 (0.0603 g, 0.215 mmol) was stirred in dichloromethane (20 mL) at room temperature overnight. The solution was allowed to filter through a small plug of Celite. The solvent was then completely removed under vacuum. The residue was washed with THF (15 mL). The white powder was collected on a frit and dried under vacuum. Crystals suitable for X-ray diffraction studies were grown by layer diffusion of MeOH into a dichloromethane solution of the compound. Yield: 0.0559 g, 52.0%; m.p. 277–279 °C; ^1H NMR (CD_2Cl_2): $\delta=1.25$ –1.97 (m, 24H; Cy-*H*), 2.17–2.25 (m, 9H; Cy-*H*), 4.63 (d, $J=14.5$ Hz, 1H; $\text{NCH}_2\text{H}_b\text{C}=\text{O}$), 5.09 (d, $J=14.1$ Hz, 1H; $\text{NCH}_2\text{H}_b\text{Ph}$), 5.96 (d, $J=14.5$ Hz, 1H; $\text{NCH}_2\text{H}_b\text{C}=\text{O}$), 6.11 (d, $J=14.1$ Hz, 1H; $\text{NCH}_2\text{H}_b\text{Ph}$), 6.84 (d, $J=2.0$ Hz, 1H; imi-*H*), 7.08 (t, $J=7.4$ Hz, 1H; Ph-*H*), 7.20 (d, $J=2.0$ Hz, 1H; imi-*H*), 7.29 (t, $J=8.0$ Hz, 2H; Ph-*H*), 7.40–7.44 (m, 3H; Ph-*H*), 7.52–7.55 (m, 2H; Ph-*H*), 7.66 (d, $J=7.4$ Hz, 2H; Ph-*H*), 9.72 ppm (brs, 1H; NH); $^{13}\text{C}\{^1\text{H}\}$ NMR (CD_2Cl_2): $\delta=26.0$ (Cy- CH_2), 27.2 (d, $^2J_{\text{PC}}=11.2$ Hz; Cy- CH_2), 30.3 (d, $^3J_{\text{PC}}=7.9$ Hz; Cy- CH_2), 37.4 (d, $^1J_{\text{PC}}=24.3$ Hz; Cy-CH), 55.6 (CH_2), 57.0 (CH_2), 119.8 (CH), 121.8 (imi-CH), 122.9 (imi-CH), 124.2 (CH), 128.6 (CH), 128.9 (CH), 129.0 (CH), 129.3 (CH), 134.0 (CH_2C), 138.1 (O=CNC), 163.2 (NCN), 164.1 ppm (C=O); $^{31}\text{P}\{^1\text{H}\}$ NMR (CD_2Cl_2): $\delta=50.8$ ppm; elemental analysis calcd (%) for $\text{C}_{36}\text{H}_{30}\text{Cl}_2\text{N}_3\text{OPPd}$: C 57.72, H 6.73, N 5.61; found: C 57.88, H 6.73, N 5.69.

Synthesis of 11: A mixture of **9** (0.123 g, 0.168 mmol) and PCy_3 (0.094 g, 0.336 mmol) was stirred in dichloromethane (25 mL) at room temperature overnight. The solvent was then completely removed under vacuum. Diethyl ether (30 mL) and THF (5 mL) were added to wash the residual solid. The white powder was collected on a frit and dried under vacuum. Crystals suitable for X-ray diffraction studies were grown by vapor diffu-

sion of diethyl ether into a dichloromethane solution of the compound. Yield: 0.125 g, 99%; m.p. 279°C (dec); ¹H NMR (CDCl₃): δ = 1.16–1.83 (m, 24H; Cy-H), 2.13–2.29 (m, 9H; Cy-H), 3.44–3.61 (m, 4H; NCH₂CH₂N), 3.80 (d, *J* = 14.4 Hz, 1H; NCH₂H₅C=O), 4.67 (d, *J* = 14.1 Hz, 1H; NCH₂H₅Ph), 5.64 (d, *J* = 14.4 Hz, 1H; NCH₂H₅C=O), 5.81 (d, *J* = 14.4 Hz, 1H; NCH₂H₅Ph), 7.08 (t, *J* = 7.5 Hz, 2H; Ph-H), 7.24–7.36 (m, 4H; Ph-H), 7.51 (d, *J* = 7.5 Hz, 2H; Ph-H), 7.74 (d, *J* = 8.1 Hz, 2H; Ph-H), 10.1 ppm (s, 1H; NH); ¹³C[¹H] NMR (CDCl₃): δ = 26.1 (Cy-CH₂), 27.4 (d, ²*J*_{PC} = 10.4 Hz; Cy-CH₂), 30.4 (d, ³*J*_{PC} = 51.3 Hz; Cy-CH₂), 37.3 (d, ¹*J*_{PC} = 23.7 Hz; Cy-CH), 47.9 (NCH₂CH₂N), 48.1 (NCH₂CH₂N), 55.8 (CH₂), 57.4 (CH₂), 120.1 (CH), 124.4 (CH), 128.6 (CH), 128.7 (CH), 129.0 (CH, two overlapping signals), 133.6 (CH₂C), 138.0 (O=CNC), 165.0 (C=O), 194.1 ppm (NCN); ³¹P[¹H] NMR (CDCl₃): δ = 49.4 ppm; elemental analysis calcd (%) for C₃₆H₅₂Cl₂N₃OPPd: C 57.56, H 6.98, N 5.59; found: C 57.26, H 7.37, N 5.29.

X-ray crystallographic data collection: Typically, the crystals were removed from the vial with a small amount of mother liquor and immediately coated with silicon grease on a weighting paper. A suitable crystal was mounted on a glass fiber with silicone grease and placed in the cold stream of a Bruker APEX II with graphite-monochromated MoK_α radiation (λ = 0.71073 Å) at 150(2) K. Crystallographic data are listed in Table 1.

Solution and structure refinements: All structures were solved by direct methods by using SHELXS-97 and refined by full-matrix least-squares methods against *F*² with SHELXL-97.^[64] Tables of neutral atom scattering factors, *f* and *f*[′], and absorption coefficients are from a standard source.^[65] There are two independent molecules of **8** in an asymmetric unit. The asymmetric unit of **9** contains a disordered CHCl₃ solvent molecule. A suitable model with three orientations (occupancy factor = 0.45, 0.4, and 0.15) was obtained by rigid-group refinement. Two orientations of the picolyl group in **7** (occupancy factor = 0.64 and 0.36) and two orientations of the imidazole ring in **10** (occupancy factor = 0.55 and 0.45) were located from the electron-density map. All atoms except hydrogen atoms were refined with anisotropic displacement parameters. In general, hydrogen atoms were fixed at calculated positions, and their positions were refined by a riding model. CCDC-687496 (**5**), 687497 (**6**), 687498 (**7**), 689768 (**8**), 687499 (**9**), 687494 (**10**), and 687495 (**11**) contain the supplementary crystallographic data for this paper. These data can be obtained free of charge from The Cambridge Crystallographic Data Centre via www.ccdc.cam.ac.uk/data_request/cif

Suzuki coupling reactions: In a typical reaction, a mixture of aryl halides (1.0 mmol), phenylboronic acid (1.5 mmol), Cs₂CO₃ (2.0 mmol), and palladium(II) precatalyst (1 mol%) in 1,4-dioxane (3 mL) was stirred at 80°C for 2 h under nitrogen. The solution was allowed to cool to ambient temperature for GC analysis. GC yields were calculated by using benzophenone as the internal standard. For isolated yields, the products were purified by column chromatography on a silica-gel column.

Computational details: We used the three-parameter hybrid of exact exchange and Becke's exchange energy functional,^[66] plus Lee, Yang, and Parr's gradient-corrected correlation energy functional (B3LYP).^[67] For the optimization of molecular geometries, we used the 6-31G basis sets for H, C, N, and O. For Pd we used the LANL2DZ effective core potential plus basis functions.^[68] The solvation free energies were computed by using the Conductor-like Polarizable Continuum Model (CPCM) of Barone and Cossi.^[53] With this method the solvation free energy of the solute embedded in a continuum medium is computed. In the CPCM model, the polarization of the solute by the solvent, and the solute–solvent dispersion–repulsion effects are included. The structures optimized in the gas-phase were used in the CPCM calculations, whereas the 6-31G(*d*) basis set is used for atoms other than Pd. We incorporated the dielectric constant of acetonitrile (ε = 36.64) in the CPCM computations. The Gaussian 03 suite of programs were used in our study.^[69]

Acknowledgements

We thank the National Science Council of Taiwan for financial support of this work. We thank the National Center for High-Performance Computing for computing time and facilities.

- [1] W. A. Herrmann, *Angew. Chem.* **2002**, *114*, 1342–1363; *Angew. Chem. Int. Ed.* **2002**, *41*, 1290–1309.
- [2] M. C. Perry, K. Burgess, *Tetrahedron: Asymmetry* **2003**, *14*, 951–961.
- [3] E. A. B. Kantchev, C. J. O'Brien, M. G. Organ, *Angew. Chem.* **2007**, *119*, 2824–2870; *Angew. Chem. Int. Ed.* **2007**, *46*, 2768–2813.
- [4] U. Christmann, R. Vilar, *Angew. Chem.* **2005**, *117*, 370–378; *Angew. Chem. Int. Ed.* **2005**, *44*, 366–374.
- [5] A. C. Hillier, G. A. Grasa, M. S. Viciu, H. M. Lee, C. Yang, S. P. Nolan, *J. Organomet. Chem.* **2002**, *653*, 69–82.
- [6] T. M. Trnka, R. H. Grubbs, *Acc. Chem. Res.* **2001**, *34*, 18–29.
- [7] S. Díez-González, S. P. Nolan, *Acc. Chem. Res.* **2008**, *41*, 349–358.
- [8] N. E. Kamber, W. Jeong, R. M. Waymouth, R. C. Pratt, B. G. G. Lohmeijer, J. L. Hedrick, *Chem. Rev.* **2007**, *107*, 5813–5840.
- [9] P. J. Barnard, S. J. Berners-Price, *Coord. Chem. Rev.* **2007**, *251*, 1889–1902.
- [10] A. Kascatan-Nebioglu, M. J. Panzner, C. A. Tessier, C. L. Cannon, W. J. Youngs, *Coord. Chem. Rev.* **2007**, *251*, 884–895.
- [11] S. Díez-González, S. P. Nolan, *Coord. Chem. Rev.* **2007**, *251*, 874–883.
- [12] L. Cavallo, A. Correa, C. Costabile, H. Jacobsen, *J. Organomet. Chem.* **2005**, *690*, 5407–5413.
- [13] O. Köhl, *Chem. Soc. Rev.* **2007**, *36*, 592–607.
- [14] H. M. Lee, C.-C. Lee, P.-Y. Cheng, *Curr. Org. Chem.* **2007**, *11*, 1491–1524.
- [15] C. Y. Liao, K. T. Chan, J. Y. Zeng, C. H. Hu, C. Y. Tu, H. M. Lee, *Organometallics* **2007**, *26*, 1692–1702.
- [16] C. Y. Liao, K. T. Chan, Y. C. Chang, C. Y. Chen, C. Y. Tu, C. H. Hu, H. M. Lee, *Organometallics* **2007**, *26*, 5826–5833.
- [17] C.-Y. Liao, K.-T. Chan, P.-L. Chiu, C.-Y. Chen, H. M. Lee, *Inorg. Chim. Acta* **2008**, *361*, 2973–2978.
- [18] N. Marion, O. Navarro, J. Mei, E. D. Stevens, N. M. Scott, S. P. Nolan, *J. Am. Chem. Soc.* **2006**, *128*, 4101–4111.
- [19] A. C. Hillier, W. J. Sommer, B. S. Yong, J. L. Petersen, L. Cavallo, S. P. Nolan, *Organometallics* **2003**, *22*, 4322–4326.
- [20] A. Labande, J.-C. Daran, E. Manoury, R. Poli, *Eur. J. Inorg. Chem.* **2007**, 1205–1209.
- [21] J. Wolf, A. Labande, J.-C. Daran, R. Poli, *Eur. J. Inorg. Chem.* **2007**, 5069–5079.
- [22] J. Wolf, A. Labande, J.-C. Daran, R. Poli, *Eur. J. Inorg. Chem.* **2008**, 3024–3030.
- [23] W. A. Herrmann, C. Köcher, L. J. Goossen, G. R. J. Artus, *Chem. Eur. J.* **1996**, *2*, 1627.
- [24] C. Yang, H. M. Lee, S. P. Nolan, *Org. Lett.* **2001**, *3*, 1511.
- [25] A.-E. Wang, J. Zhong, J.-H. Xie, K. Li, Q.-L. Zhou, *Adv. Synth. Catal.* **2004**, *346*, 595.
- [26] N. Tsoureas, A. A. Danopoulos, A. A. D. Tulloch, M. E. Light, *Organometallics* **2003**, *22*, 4750–4758.
- [27] C.-C. Lee, W.-C. Ke, K.-T. Chan, C.-L. Lai, C.-H. Hu, H. M. Lee, *Chem. Eur. J.* **2007**, *13*, 582–591.
- [28] H. M. Lee, J. Y. Zeng, C.-H. Hu, M.-T. Lee, *Inorg. Chem.* **2004**, *43*, 6822–6829.
- [29] K. Albert, P. Gisdakis, N. Rosch, *Organometallics* **1998**, *17*, 1608–1616.
- [30] W. A. Herrmann, V. P. W. Böhm, C. W. K. Gstöttmayr, M. Grosche, C.-P. Reisinger, T. Weskamp, *J. Organomet. Chem.* **2001**, *617*–618, 616–628.
- [31] R. Cowdell, C. J. Davies, S. J. Hilton, J.-D. Marechal, G. A. Solan, O. Thomas, J. Fawcett, *Dalton Trans.* **2004**, 3231–3240.
- [32] M. Süßner, H. Plenio, *Chem. Commun.* **2005**, 5417–5419.
- [33] S. Leuthäuser, D. Schwarz, H. Plenio, *Chem. Eur. J.* **2007**, *13*, 7195–7203.

- [34] P. D. Stevens, J. Fan, H. M. R. Gardimalla, M. Yen, Y. Gao, *Org. Lett.* **2005**, *7*, 2085–2088.
- [35] S. Tandukar, A. Sen, *J. Mol. Catal. A: Chem.* **2007**, *268*, 112–119.
- [36] M. A. Kalam, K. Haraguchi, S. Chandani, E. L. Loechler, M. Moriya, M. M. Greenberg, A. K. Basu, *Nucl. Acids Res.* **2006**, *34*, 2305–2315.
- [37] N. Nakanishi, F. Takeuchi, H. Okamoto, A. Tamura, H. Hori, M. Tsubaki, *J. Biochem.* **2006**, *140*, 561–571.
- [38] Z. Zhang, H. Lönberg, S. Mikkola, *Chem. Biodiversity* **2005**, *2*, 92.
- [39] B. Tudek, *J. Biochem. Mol. Biol.* **2003**, *36*, 12.
- [40] M. K. Denk, J. M. Rodezno, S. Gupta, A. J. Lough, *J. Organomet. Chem.* **2001**, *617–618*, 242–253.
- [41] A. W. Waltman, T. Ritter, R. H. Grubbs, *Organometallics* **2006**, *25*, 4238–4239.
- [42] A. W. Waltman, R. H. Grubbs, *Organometallics* **2004**, *23*, 3105–3107.
- [43] G. C. Lloyd-Jones, R. W. Alder, G. J. J. Owen-Smith, *Chem. Eur. J.* **2006**, *12*, 5361–5375.
- [44] Y. Matsuoka, Y. Ishida, K. Saigo, *Tetrahedron Lett.* **2008**, *49*, 2985–2989.
- [45] E. Despagnet-Ayoub, R. H. Grubbs, *Organometallics* **2005**, *24*, 338–340.
- [46] D. Kremzow, G. Seidel, C. W. Lehmann, A. Fürstner, *Chem. Eur. J.* **2005**, *11*, 1833–1853.
- [47] H. V. Huynh, Y. Han, J. H. H. Ho, G. K. Tan, *Organometallics* **2006**, *25*, 3267–3274.
- [48] H. V. Huynh, C. H. Yeo, G. K. Tan, *Chem. Commun.* **2006**, 3833–3835.
- [49] R. A. Batey, M. Shen, A. J. Lough, *Org. Lett.* **2002**, *4*, 1411–1414.
- [50] L. R. Titcomb, S. Caddick, F. G. N. Cloke, D. J. Wilson, D. McKercher, *Chem. Commun.* **2001**, 1388–1389.
- [51] M. Heckenroth, E. Kluser, A. Neels, M. Albrecht, *Angew. Chem.* **2007**, *119*, 6409–6412; *Angew. Chem. Int. Ed.* **2007**, *46*, 6293–6296.
- [52] J. F. Moulder, W. F. Stickle, P. E. Sobol, K. D. Bomben, *Handbook of X-ray Photoelectron Spectroscopy*, Perkin-Elmer Corporation, Minnesota, **1992**.
- [53] V. Barone, M. Cossi, *J. Phys. Chem. A* **1998**, *102*, 1995–2001.
- [54] M. Trilla, R. Pleixats, M. W. C. Man, C. Bied, J. J. E. Moreau, *Adv. Synth. Catal.* **2008**, *350*, 577–590.
- [55] V. Polshettiwar, R. S. Varma, *Tetrahedron* **2008**, *64*, 4637–4643.
- [56] J. J. E. Hardy, S. Hubert, D. J. Macquarrie, A. J. Wilson, *Green Chem.* **2004**, *6*, 53–56.
- [57] K. Albert, P. Gisdakis, N. Rösch, *Organometallics* **1998**, *17*, 1608–1616.
- [58] A. Gniewek, J. J. Ziolkowski, A. M. Trzeciak, M. Zawadzki, H. Grabowska, J. Wrzyszczyk, *J. Catal.* **2008**, *254*, 121–130.
- [59] J. A. Widegren, R. G. Finke, *J. Mol. Catal. A: Chem.* **2003**, *198*, 317–341.
- [60] G. M. Whitesides, M. Hackett, R. L. Brainard, J. P. P. M. Lavalleye, A. F. Sowinski, A. N. Izumi, S. S. Moore, D. W. Brown, E. M. Staudt, *Organometallics* **1985**, *4*, 1819–1830.
- [61] P. Foley, R. DiCosimo, G. M. Whitesides, *J. Am. Chem. Soc.* **1980**, *102*, 6713–6725.
- [62] C. J. O'Brien, E. A. B. Kantchev, C. Valente, N. Hadei, G. A. Chass, A. J. Lough, A. C. Hopkinson, M. G. Organ, *Chem. Eur. J.* **2006**, *12*, 4743–4748.
- [63] W. L. F. Armarego, C. L. L. Chai, *Purification of Laboratory Chemicals*, 5th ed., Elsevier Science, Burlington, **2003**.
- [64] G. M. Sheldrick, *SHELXTL*, 5.1 ed., Bruker AXS Inc., Madison, Wisconsin, **1998**.
- [65] L. E. Sutton, *Tables of Interatomic Distances and Configurations in Molecules and Ions*, Chemical Society Publications, U.K., **1965**.
- [66] A. D. Becke, *J. Chem. Phys.* **1993**, *98*, 5648.
- [67] C. Lee, W. Yang, R. G. Parr, *Phys. Rev. B* **1988**, *37*, 785.
- [68] P. J. Hay, W. R. Wadt, *J. Chem. Phys.* **1985**, *82*, 270.
- [69] Gaussian 03, Revision B.05, M. J. Frisch, G. W. Trucks, H. B. Schlegel, G. E. Scuseria, M. A. Robb, J. R. Cheeseman, J. A. Montgomery, Jr., T. Vreven, K. N. Kudin, J. C. Burant, J. M. Millam, S. S. Lyengar, J. Tomasi, V. Barone, B. Mennucci, M. Cossi, G. Scalmani, N. Rega, G. A. Petersson, H. Nakatsuji, M. Hada, M. Ehara, K. Toyota, R. Fukuda, J. Hasegawa, M. Ishida, T. M. Nakajima, Y. Honda, O. Kitao, H. Nakai, M. Klene, X. Li, J. E. Knox, H. P. Hratchian, J. B. Cross, C. Adamo, J. Jaramillo, R. Gomperts, R. E. Stratmann, O. Yazyev, A. J. Austin, R. Cammi, C. Pomelli, J. Ochterski, P. Y. Ayala, K. Morokuma, G. A. Voth, P. Salvador, J. J. Dannenberg, V. G. Zakrzewski, S. Dapprich, A. D. Daniels, M. C. Strain, O. Farkas, D. K. Malick, A. D. Rabuck, K. Raghavachari, J. B. Foresman, J. V. Ortiz, Q. Cui, A. G. Baboul, S. Clifford, J. Cioslowski, B. B. Stefanov, G. Liu, A. Liashenko, P. Piskorz, I. Komaromi, R. L. Martin, D. J. Fox, T. Keith, M. A. Al-Laham, C. Y. Peng, A. Nanayakkara, M. Challacombe, P. M. W. Gill, B. Johnson, W. Chen, M. W. Wong, C. Gonzalez, J. A. Pople, Gaussian, Inc., Pittsburgh PA, **2003**.

Received: June 28, 2008
Published online: November 26, 2008